DOI: 10.5185/amlett.2025.021777

RESEARCH



Microstructural Investigation of Commercial Ayurvedic Bhasma Samples by Optical, UV-visible and FTIR Analyses

Bimal Rajchal^{1,2,3,4}, Yub Narayan Thapa^{1,3,4,5}, Deepshikha Karki^{1,3,4}, Ramesh Puri^{3,4}, Pramod Bhatta ⁶, Motee Lal Sharma^{1,3}, Vimal Katiyar⁷, Rameshwar Adhikari^{1,3,4,7,*}

¹Central Department of Chemistry, Tribhuvan University, Kirtipur 44618, Bagmati Province, Nepal ²Bhaktapur Multiple Campus, Tribhuvan University, Bhaktapur 44800, Bagmati Province, Nepal ³Nepal Polymer Institute (NPI), Kathmandu 44618, Bagmati Province, Nepal ⁴Research Centre for Applied Science and Technology (RECAST), Tribhuvan University, Kirtipur 44618, Bagmati Province, Nepal ⁵Tribhuvan Multiple Campus, Tribhuvan University, Tansen, Palpa 32500, Lumbini Province, Nepal ⁶Vidushi Yogamaya Himalayan Ayurveda University, Sankhuwasabha 56900, Koshi Province, Nepal ⁷Indian Institute of Technology Guwahati, Guwahati 781039, Assam,

*Corresponding author:

E-mail: nepalpolymer@yahoo.com Tel.: +977-9841390927

ABSTRACT

Ayurvedic Bhasmas, the traditional metallic and mineral-based formulations with therapeutic properties, are used to manage various human ailments in Ayurveda. Despite their therapeutic applications, the scientific validation of their physicochemical properties remains limited. This study aims to characterize and better understand selected commercially available Bhasmas through optical microscopic and different spectroscopic techniques, providing insights into their structural and compositional attributes. Optical microscopy revealed their irregular morphology and powdery texture with heterogeneous particle sizes. Ultraviolet – visible (UV-visible) spectroscopy showed absorption peaks between 257 nm and 390 nm, and band gap energies between 1.94 eV and 5.36 eV, suggesting the presence of nanosized particles. Fourier Transform Infrared spectroscopy (FTIR) revealed the presence of organic moieties and metal-oxygen bonds within the Bhasma samples, indicating possible herbal interactions with metallic or mineral components during their preparation. These findings support the notion that Bhasmas possess unique physicochemical features, potentially contributing to their therapeutic efficacy.

KEYWORDS

Ayurveda, Bhasma, Vedic medicine, Ayurvedic formulation, Traditional nanomedicine, Calx

INTRODUCTION

Originated in the Indian sub-continent regions more than 5000 years ago, Ayurveda, the traditional healthcare system, amalgamates Vedic science with philosophy of life, offering a holistic medical approach to living a healthier, happier, and more prosperous life through a variety of therapies [1,2]. The *Ayurvedic* doctrine holds that *Tridoshas* (Three States) and *Saptadhatus* (Seven Tissues) formed through unique combination and proportion of *Pancha Mahbhootas* (Five fundamental elements) determine health condition of each individual [3]. *Vayu* (Air), *Jala* (Water), *Prithvi* (Earth), *Teja or Agni* (Fire), and *Akash* (space or ether) are the five fundamental elements that undergo combination in various ways and ratio to form the three doshas: *Vata dosha* (Air and Space), *Pitta dosha*

(Fire and Water), and *Kapha dosha* (Water and Earth), and the seven tissues: *Rasa* (Fluids or Plasma), *Rakta* (Blood), *Mamsa* (Muscles), *Meda* (Fats and Connectives), *Asthi* (Bones), *Majja* (Marrow), and *Shukra* (Semen) [4]. The imbalance in *doshas* and *dhatus*, triggered by seasonal variations, misuse of senses, and misuse of intellect, creates health abnormalities, and is corrected by supplying a suitable dose of *Ayurvedic* medicines [5].

Having a longer shelf life and nanoscale dimensions, *Ayurvedic Bhasmas* resemble such Vedic medicines and are highly effective and efficient in action. These are one of the classical *Ayurvedic* formulations in the form of fine ash that contain non-toxic forms of metals and minerals as major therapeutic ingredients along with carbonaceous particles [6]. The systematic and stepwise procedure of *Bhasma* preparation is well described in *Ayurvedic* scriptures and

This is an open access article licensed under the Creative Commons Attribution 4.0 International License, which allows for use, distribution, and reproduction in any medium as long as the original work is properly cited. The Authors © 2025. The International Association of Advanced Materials, Sweden, publishes Advanced Materials Letters.



the process is called 'Bhasmikaran' (Transformation into calx) [7]. Similar to tribochemistry [8], the Bhasmikaran process involves mechanochemical processing of metals or minerals followed by high-temperature treatment to reduce particle size effectively and to transform the toxic nature of metals and minerals into a non-toxic form with enhanced therapeutic value and efficacy [9–11]. In Ayurvedic treatment, different Bhasmas are recommended for the treatment of various diseases, including chronic diseases like cancer, asthma, gastritis, and others. Recent studies claim that Bhasmas are the traditional equivalent of modern nanomedicine, which have antioxidant, anti-inflammatory, immunomodulatory, antibacterial, antiviral and antitumor properties [12,13].

Different microscopic and spectroscopic techniques are used to characterize *Bhasmas*. This paper only focusses on optical microscopy, UV-visible spectroscopy and FTIR spectroscopy of ten commercial Bhasmas. Optical microscope, also called light microscope, is versatile and the first-line microscopy option to generate magnified image of specimen by utilizing visible light and system of lenses with magnification 50x to 1000x. It is affordable, easy to use and flexible technique offering wide magnification range and high-resolution images. The optical microscopy of Ayurvedic Bhasmas provides a preliminary idea about the micro-constituents and structure of the materials [14]. Spectroscopic methods provide useful information on the composition and structure of materials by studying the interaction of matter with electromagnetic radiation. UV-visible spectroscopy of *Bhasmas* gives invaluable insights into their optical properties by studying matter-light interaction in the visible and ultraviolet regions of the electromagnetic spectrum. Similarly, FTIR spectroscopy helps identifying various functional groups incorporated in Bhasmas by studying matter-light interaction in the infrared region of the electromagnetic spectrum [15].

EXPERIMENTAL

Sample collection and identification

Ten samples of different *Bhasmas* were purchased from the vendor. The list of samples along with their Chemical name, manufacture date, and reference of manufactured method as labelled in the samples is given in **Table 1**.

Samples characterization

Optical microscopy

The magnified images of *Bhasma* samples were obtained by using a bright field condenser optical microscope, Boeco Binocular microscope – BM – 700 (Germany), under 10x, 40x and 100x objective lens magnification. The images were captured using a B-CAM Microscope Camera attached to the microscope and B-View software integrated with camera control. The average particle size was calculated from the image (40x magnification) using ImageJ software.

Table 1. List of commercial *Ayurvedic Bhasma* samples.

Chemical name	Manufacture date	Manufactured under reference
Incinerated mica	07/2021	Ayurveda Prakash 2
Iron	08/2020	Bharat Bhaishajya Ratnakar 4/6416
Coral	09/2020	Rasatarangini 23/134 – 135
Silver	02/2022	Rasatarangini 16/26 – 28
Conch shell	01/2021	Rasatarangini 12/17 – 19
Copper pyrite	07/2020	Rasa Chandanshu 176
Copper	11/2021	Rasaratna Samuchchaya 5/53
Lead, Tin and Zinc incinerated together	03/2022	Bharat Bhaishajya Ratnakar 2/2758
Tin	03/2024	Rasatarangini 18/15 – 18
Zinc	03/2024	Rasatarangini 19/104 – 107
	Incinerated mica Iron Coral Silver Conch shell Copper pyrite Copper Lead, Tin and Zinc incinerated together Tin	name date Incinerated mica 07/2021 Iron 08/2020 Coral 09/2020 Silver 02/2022 Conch shell 01/2021 Copper pyrite 07/2020 Copper incinerated together 03/2022 Tin 03/2024

UV-visible spectroscopy

The optical absorption spectra of collected *Bhasma* samples were obtained by the UV 1900 Shimadzu (USA) UV-visible spectrophotometer. A total of 1 mg of each sample was dispersed in 10 mL of deionized water, sonicated for 2 minutes and the spectrum was recorded in the range of 200 – 600 nm. The data were subsequently collected and graphs were generated using Origin Pro software. The data were also used to obtain Tauc plot using Origin Pro software to calculate band gap energy.

The Tauc plot relation is expressed as,

$$(\alpha h \upsilon)^n = K(h \upsilon - E_{\sigma})$$

Where, ' α ' is absorption coefficient, ' θ ' is incident photon energy, 'K' is an energy independent constant, ' θ ' is the band gap energy and ' θ ' is the nature of transitions which can take values 2 (for direct allowed transition) or ½ (for indirect allowed transition).

In the Tauc plot, 'hu' (in eV) is plotted on x-axis and $(\alpha h u)^n$ (in eVcm⁻¹)ⁿ on y-axis.

'hu' is calculated using the relation hu = $\frac{1240}{\text{Wavelength}}$ and $(\alpha \text{hu})^n$ is calculated using the relation

$$(\alpha h \upsilon)^n = (2.303 \times Absorbance \times h \upsilon)^n$$

A straight line is drawn through the linear part of the curve in the plot and extrapolated towards x-axis to get band gap energy value.

OPEN ACCESS

FTIR spectroscopy

FTIR spectroscopy of the samples was performed with IRAffinity-1S Shimadzu (Japan) FTIR spectrophotometer. Each sample was scanned (40 scans) from 4000 to 400cm⁻¹ at a resolution of 4 cm⁻¹ in an attenuated total reflection (ATR) mode. The data was subsequently collected and graphs were generated using Origin Pro software.

RESULTS AND DISCUSSION

Abhrak Bhasma

Abhrak Bhasma exhibited a powdery texture with an average particle size of 28.5 µm as observed under light microscopy (Fig. 1A). The UV-visible spectrum of Abhrak Bhasma (Fig. 1B) displayed a broad absorption band at 257 nm, which may suggest the presence of nanosized silicate particles derived from biotite mineral, consistent with the known silicate absorption near 297 nm reported in the literature [16]. The band gap energy of Abhrak Bhasma was obtained from the Tauc plot (Fig. 1C) as 3.01 eV, suggesting the presence of nanosized particles. This observation is in close agreement to the band gap energy of pure silica (3.85 eV) as reported in earlier literature [17]. The FTIR spectrum of Abhrak Bhasma (Fig. 1D), showed distinct peaks centered around 2920 cm⁻¹ and 2850 cm⁻¹, corresponding to O-H stretching vibrations, indicating the presence of Mg-OH and Al-OH groups and suggesting its hydrophilic nature. A Peak at 1745 cm⁻¹ is attributed to the O=C=O stretching vibrations of carbon dioxide or carbonate groups. The characteristic peak centered at 951 cm⁻¹ is linked to Si-O stretching vibrations, suggesting the presence of silicate structures, while the peaks at 680 cm⁻¹ and 590 cm⁻¹ are ascribed to C-S and S-S stretching vibrations, respectively [18,19].

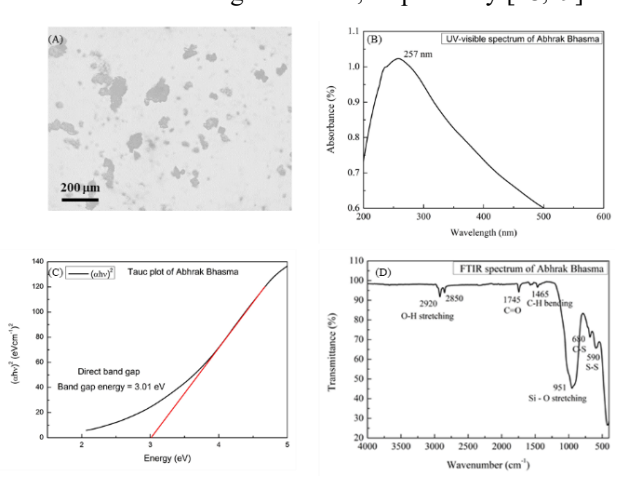


Fig. 1. Optical microscopy image (A), UV-visible spectrum (B), Tauc plot (C) and FTIR spectrum (D) of *Abhrak Bhasma*.

Loha Bhasma

Loha Bhasma showed a powdery morphology with an average particle size of 23.5 μm as seen under optical microscopy (Fig. 2A). In UV-visible spectrum (Fig. 2B), a

minor absorption peak at 356 nm was observed which corresponds to iron oxide nanoparticles, aligning well with the 340 nm band reported for iron oxide [20]. The band gap energy of *Loha Bhasma*, calculated from the Tauc plot (Fig. 2C), was found to be 5.12 eV, indicating the presence of nanoparticles. However, the band gap value for iron oxide nanoparticles is reported to be 2.60 eV in previous study [21]. The FTIR spectrum of *Loha Bhasma* (Fig. 2D) displayed prominent peaks at 526 and 432 cm⁻¹, which are indicative of Fe-O vibrations associated with iron oxides [22,23].

Praval Bhasma

The optical microscopy image (**Fig. 3A**) of *Praval Bhasma* displayed powdery texture with an average particle size of 20.1 µm. In UV-visible spectrum (**Fig. 3B**), *Praval Bhasma* revealed a broad absorption peak at 335 nm, which is consistent with the reported peak of green synthesized calcium oxide (CaO) nanoparticles [24], indicating the presence of calcium oxide. The band gap energy of *Praval Bhasma*, calculated from the Tauc plot (**Fig. 3C**), was found to be 4.65 eV, indicating the presence of nanoparticles.

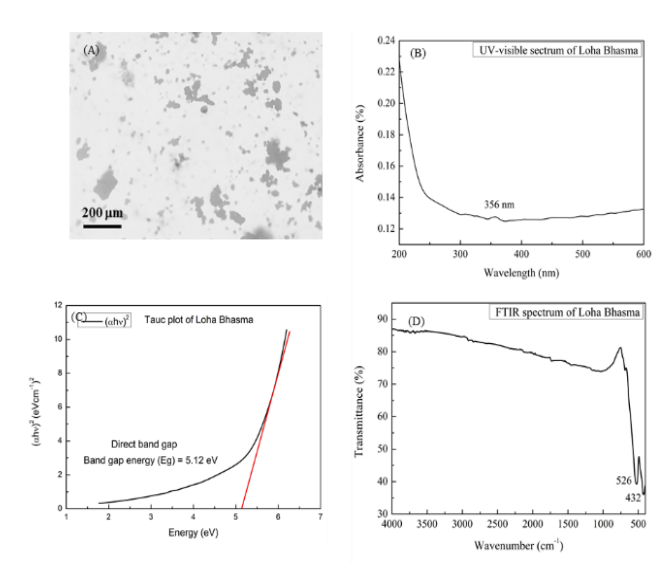


Fig. 2. Optical microscopy image (A), UV-visible spectrum (B), Tauc plot (C) and FTIR spectrum (D) of *Loha Bhasma*.

The band gap energy value is in close agreement with that of calcium oxide nanoparticles (4.22 eV) reported in the previous literature [25]. In the FTIR spectrum of *Praval Bhasma* (Fig. 3D), a peak centered at 3690 cm⁻¹ corresponds to O-H stretching vibrations, indicating the presence of moisture in the *Bhasma*. The peaks at 2510 cm⁻¹ and 1795 cm⁻¹ are associated with C-H stretching and C=O stretching vibrations, respectively. The prominent peaks centered around 1400 cm⁻¹, 873 cm⁻¹ and 710 cm⁻¹ represent symmetric and asymmetric CO₃²⁻ vibrations, characteristic of the calcite form of calcium carbonate. The additional peak at 490 cm⁻¹ is indicative of the presence of Ca-O bonds [26–28].



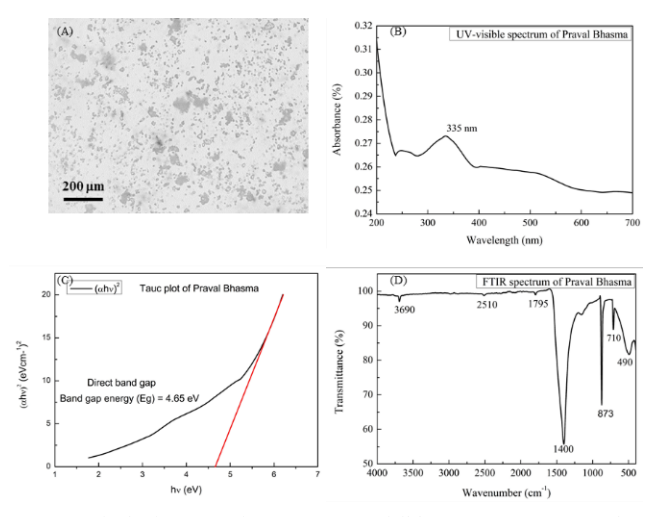


Fig. 3. Optical microscopy image (A), UV-visible spectrum (B), Tauc plot (C) and FTIR spectrum (D) of *Praval Bhasma*.

Rajat Bhasma

The optical microscopy image of Rajat Bhasma (Fig. 4A) exhibited a powdery texture with average particle size of 31.2 µm. While silver nanoparticles typically exhibit a surface plasmon resonance near 420 nm [29], the absorption band for Rajat Bhasma appeared at 338 nm in its UV-visible spectrum (Fig. 4B), suggesting the likely presence of other metallic particles rather than pure silver nanoparticles. The band gap energy of Rajat Bhasma, calculated from the Tauc plot (Fig. 4C), was found to be 1.94 eV, indicating the presence of nanoparticles. The calculated band gap energy is very close to that of green synthesized silver oxide nanoparticles (2.1 eV) reported in the previous studies [30]. In the FTIR spectrum of Rajat Bhasma (Fig. 4D), a broad band between 3700 and 3900 cm⁻¹ corresponds to O-H stretching vibrations. A Peak at 1460 cm⁻¹ is attributed to CH₂ bending vibrations, while the peak centered at 408 cm⁻¹ is associated with Ag-O bonding [31,32].

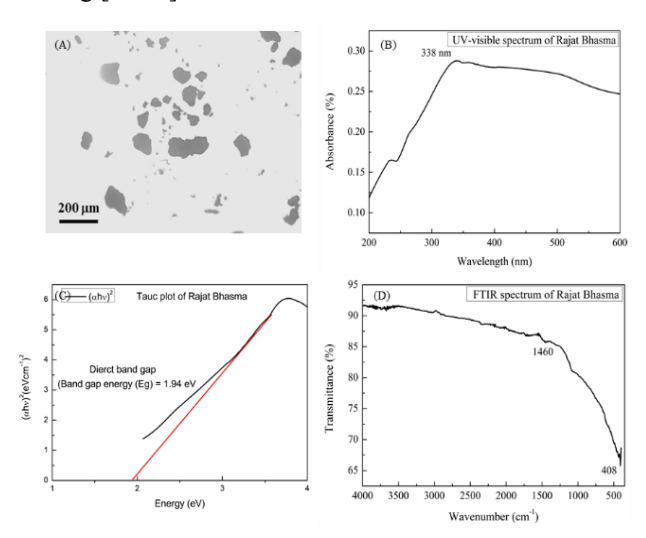


Fig. 4. Optical microscopy image (A), UV-visible spectrum (B), Tauc plot (C) and FTIR spectrum (D) of *Rajat Bhasma*.

Sankha Bhasma

Sankha Bhasma exhibited a fine powdery texture with an average particle size of 14.7 µm, as observed in the optical microscopy image (Fig. 5A). The distinct absorption band at 336 nm observed for Sankha Bhasma in UV-visible spectrum (Fig. 5B) points to the presence of calcium oxide nanoparticles, as noted in previous studies [24]. The band gap energy of Sankha Bhasma, calculated from the Tauc plot (Fig. 5C), was found to be 4.85 eV, indicating the presence of nanoparticles. The calculated band gap energy is very close to that of calcium oxide nanoparticles (4.22 eV) reported in earlier studies [25]. The FTIR spectrum of Sankha Bhasma (Fig. 5D) closely resembles that of Praval Bhasma. The peak centered at 3640 cm⁻¹ corresponds to O-H stretching vibrations, signifying moisture content. The prominent peaks at 1415 cm⁻¹, 874 cm⁻¹ and 712 cm⁻¹ are characteristic of the calcite form of calcium carbonate, and the additional peak at 425 cm⁻¹ confirms the presence of Ca-O bonds [33,34].

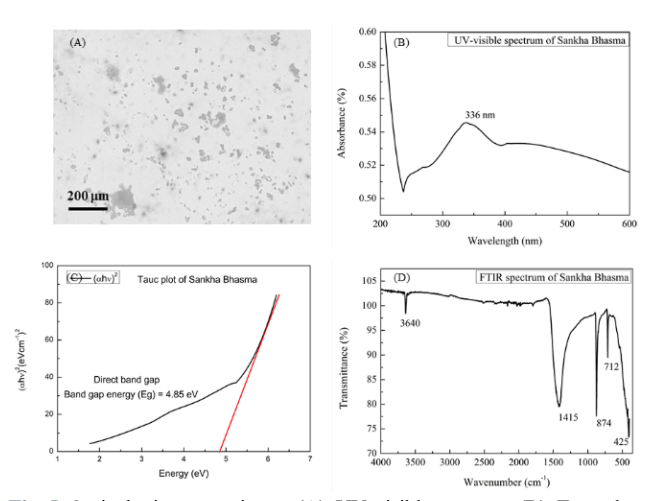


Fig. 5. Optical microscopy image (A), UV-visible spectrum (B), Tauc plot (C) and FTIR spectrum (D) of *Sankha Bhasma*

Suvarnamakshik Bhasma

Suvarnamakshik Bhasma showed a powdery texture with an average particle size of 30 μm, as observed under optical microscopy image (**Fig. 6A**). The UV-visible spectrum (**Fig. 6B**) displayed an absorption peak at 310 nm, which corresponds to the presence of iron sulphide (285 nm) and copper sulphide (287 nm) nanoparticles, consistent with findings from previous research [35,36].

The band gap energy of Suvarnamakshik Bhasma was obtained from the Tauc plot (Fig. 6C) as 5.25 eV, suggesting the presence of nanosized particles. The band gap energy does not match that of iron sulphide nanoparticles (4.36 eV) and copper sulphide nanoparticles (2.31 eV) reported in the earlier studies [37,38] but the result is close to the value found for Loha Bhasma (5.12 eV) and Tamra Bhasma (5.36 eV), suggesting the presence of iron oxide and copper oxide nanoparticles. This is supported by the FTIR spectrum of Suvarnamakshik



Bhasma (**Fig. 6D**). In FTIR spectrum, a peak at 1069 cm⁻¹ corresponds to C-O stretching vibrations, while the peaks at 528 cm⁻¹ and 439 cm⁻¹ are attributed to Fe-O and Cu-O bonds, respectively [**39**].

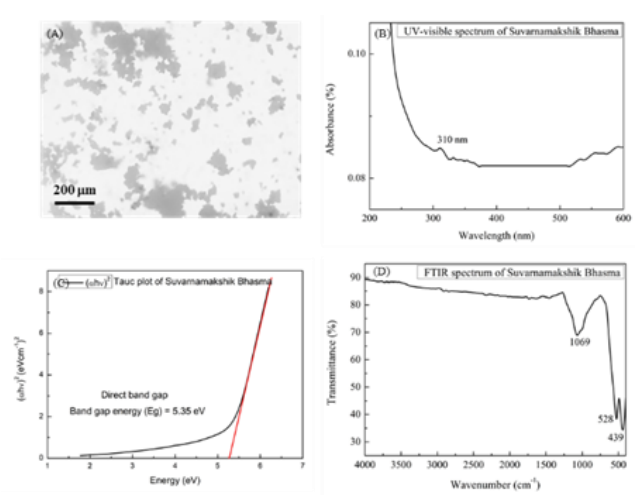


Fig. 6. Optical microscopy image (A), UV-visible spectrum (B), Tauc plot (C) and FTIR spectrum (D) of *Suvarnamakshik Bhasma*

Tamra Bhasma

Tamra Bhasma appeared as a fine powder with an average particle size of 18.6 μm, as observed in the optical microscopy image (**Fig. 7A**). Tamra Bhasma showed an absorption bands at 340 and 460 nm in the UV-visible spectrum (**Fig. 7B**), which can be attributed to cupric oxide nanoparticles and is closely aligned with the CuO absorption band at 360 nm reported in the literature [40]. The band gap energy of Tamra Bhasma was obtained from the Tauc plot (**Fig. 7C**) as 5.36 eV, suggesting the presence of nanosized particles. However, band gap energy for copper oxide nanoparticles is reported as 2.74 eV in earlier studies [41]. The FTIR spectrum of Tamra Bhasma (**Fig. 7D**) displayed O-H stretching vibration band around 3735 cm⁻¹, a C-O stretching vibration at 1056 cm⁻¹, and a characteristic Cu-O bond peak at 430 cm⁻¹ [42].

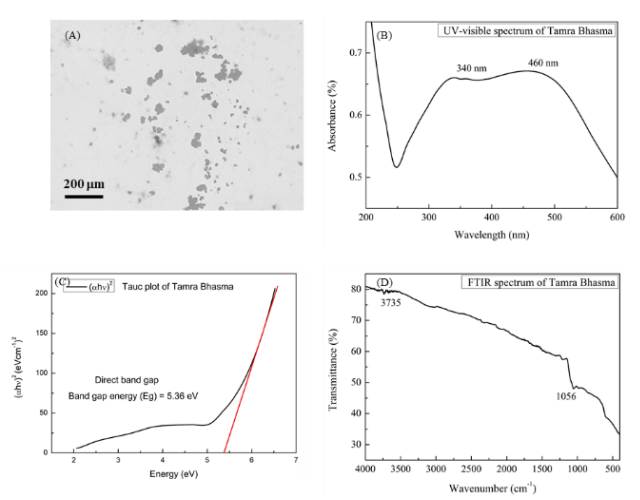


Fig. 7. Optical microscopy image (A), UV-visible spectrum (B), Tauc plot (C) and FTIR spectrum (D) of *Tamra Bhasma*

Trivanga Bhasma

Trivanga Bhasma showed a powdery texture with an average particle size of 37.2 µm, as seen in the optical microscopy image (Fig. 8A). Trivanga Bhasma exhibited three distinct bands at 214, 248 and 322 nm in the UVvisible spectrum (Fig. 8B), indicating the presence of nanosized forms of lead, tin, and zinc compounds, respectively. These findings correlate with reported absorption bands for lead oxide nanoparticles at 230 nm [43], tin oxide nanoparticles at around 250 nm [44] and zinc oxide nanoparticles at 367 nm [45]. The band gap energy of Trivanga Bhasma was obtained from the Tauc plot (Fig. 8C) as 5.35 eV, suggesting the presence of nanosized particles. The calculated band gap energy is much closer to that of lead oxide nanoparticles (5.52 eV) [46] but much greater than that for tin oxide nanoparticles (3.02 eV) [47] and zinc oxide nanoparticles (3.26 eV) reported in earlier studies [48]. In the FTIR spectrum of Trivanga Bhasma (Fig. 8D), peaks at 2340 cm⁻¹, 1463 cm⁻¹ and 1039 cm⁻¹ correspond to the asymmetric stretching vibration of CO₂ molecule, CH₂ bending vibrations and C-O stretching vibrations, respectively. Additionally, peaks at 593 cm⁻¹ and 471cm⁻¹ are attributed to Sn-O and Cu-O bonds, respectively [42,49].

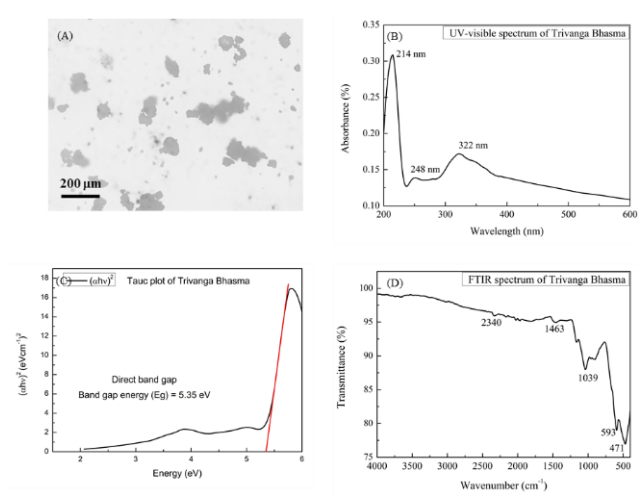


Fig. 8. Optical microscopy image (A), UV-visible spectrum (B), Tauc plot (C) and FTIR spectrum (D) of *Trivanga Bhasma*

Vanga Bhasma

Vanga Bhasma showed a powdery texture with an average particle size of 30.5 μm, as seen in the optical microscopy image (**Fig. 9A**). In the UV-visible spectrum of *Vanga Bhasma* (**Fig. 9B**), absorption band at 290 nm was observed, consistent with the presence of tin oxide nanoparticles as previously noted [44], while an additional absorption band at 390 nm may suggest copper oxide nanoparticle impurities [40].

The band gap energy of *Vanga Bhasma*, calculated from the Tauc plot (**Fig. 9C**), was found to be 4.47 eV, indicating the presence of nanoparticles. Band gap energy for tin oxide nanoparticles is, however, reported to be



3.02 eV in previous literature [47]. In the FTIR spectrum of *Vanga Bhasma* (**Fig. 9D**), a peak at 605 cm⁻¹ corresponds to the characteristic Sn-O bond [49]. The peak at 459 cm⁻¹ is indicative of the presence of Cu-O bonds, further supporting the UV-visible findings of copper oxide content.

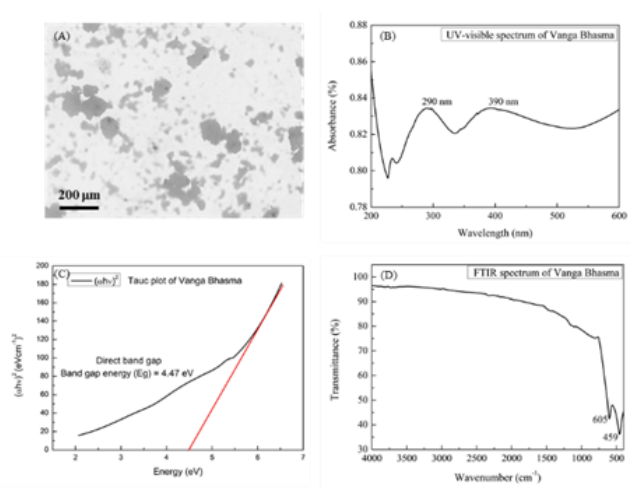


Fig. 9. Optical microscopy image (A), UV-visible spectrum (B), Tauc plot (C) and FTIR spectrum (D) of *Vanga Bhasma*

Yashad Bhasma

Yashad Bhasma appeared as a powder with an average particle size of 28 μm, as observed in the optical microscopy image (Fig. 10A). Yashad Bhasma revealed a notable peak at 347 nm in the UV-visible spectrum (Fig. 10B), which corresponds well with the zinc oxide nanoparticle absorption band at 367 nm reported in the literature [45]. The band gap energy of Yashad Bhasma, calculated from the Tauc plot (Fig. 10C), was found to be 4.85 eV, indicating the presence of nanoparticles. However, band gap energy for zinc oxide nanoparticles is reported as 3.26 eV in the earlier literature [48]. The FTIR spectrum of Yashad Bhasma (Fig. 10D) displayed peaks at 1466 cm⁻¹, 887 cm⁻¹, and 419 cm⁻¹, associated with CH₂ bending vibrations, C-O stretching vibrations, and Zn-O bond, respectively [50].

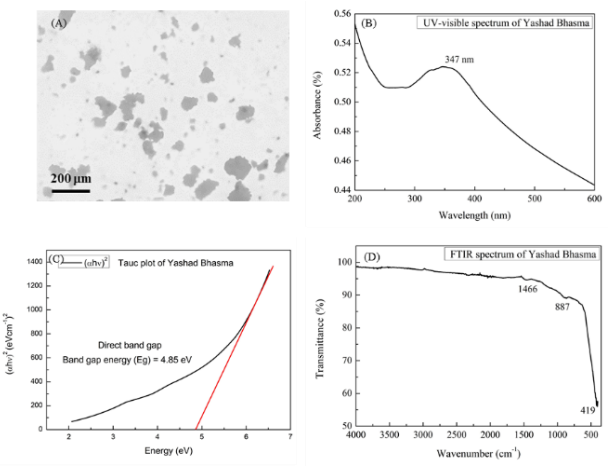


Fig. 10. Optical microscopy image (A), UV-visible spectrum (B), Tauc plot (C) and FTIR spectrum (D) of Yashad Bhasma

Summary

Optical microscopy images of the *Bhasmas* revealed that the *Bhasma* particles have powdery morphology with average particle sizes falling within the micrometer range. UV-visible spectroscopy of those *Bhasmas* detected absorption peaks ranging from 257 to 390 nm, suggesting the presence of nanosized particles. This observation is supported by the calculation of band gap energy using the Tauc plot. The band gap energy of those *Bhasmas* lies in the range of 1.94 to 5.36 eV. Additionally, FTIR analysis confirmed the presence of various organic moieties and metal-oxygen bonds in the *Bhasma* samples. A detailed summary of the observations is depicted in Supporting **Table S1**.

CONCLUSION

present study provides a comprehensive physicochemical evaluation of commercially available Ayurvedic Bhasmas using optical microscopy, UV-visible spectroscopy, and FTIR analysis. Optical microscopy revealed heterogeneous particle sizes and powdery textures, indicating the presence of micro- to nanoscale particles. UV-visible spectroscopy showed characteristic absorption patterns and band gap energies suggestive of nanosized particles with potential therapeutic relevance. FTIR analysis revealed the presence of metal-oxygen bonds and organic functional groups, reflecting possible herbal interactions with metallic or mineral components of Bhasmas during their preparation. Overall, the combined microscopic and spectroscopic results emphasize the unique structural and chemical features of Ayurvedic Bhasmas, supporting their classification as traditional nanomedicine. Further standardization and in-depth characterization are, however, essential to ensure their consistency, safety, and efficacy in clinical applications.

ACKNOWLEDGEMENTS

We are also thankful to Bhaktapur Multiple Campus, Bhaktapur, for providing study leave facilities to BR. We gratefully acknowledge the Centre for International Migration and Development (CIM), Germany, for the support of the Optical Microscope and UV-Vis. Spectrophotometer as a part of the return fellowship to Mr. Ramesh Puri.

CONFLICTS OF INTEREST

There are no conflicts to declare.

REFERENCES

- A. Kizhakkeveettil, J. Parla, K. Patwardhan, A. Sharma, S. Sharma, History, Present and Prospect of Ayurveda, in: Hist. Present Prospect World Tradit. Med., World Scientific Publishing Co., 2023: pp. 1– 72. https://doi.org/10.1142/9789811282171 0001.
- P.K. Mukherjee, R.K. Harwansh, S. Bahadur, S. Banerjee, A. Kar, J. Chanda, S. Biswas, S.M. Ahmmed, C.K. Katiyar, Development of Ayurveda Tradition to trend, *J. Ethnopharmacol.*, 2017, 197, 10–24. https://doi.org/10.1016/J.JEP.2016.09.024.
- M. Heinrich, J. Barnes, S. Gibbons, E.M. Williamson, Fundamentals of pharmacognosy and phytotherapy, 2nd ed., Elsevier Ltd, 2012.
- Y.S. Jaiswal, L.L. Williams, A glimpse of Ayurveda The forgotten history and principles of Indian traditional medicine, J. Tradit.

Advanced Materials Letters

https://aml.iaamonline.org

OPEN ACCESS

- Complement. Med., **2016**, 7, 50. https://doi.org/10.1016/J.JTCME.2016.02.002.
- B. Ravishankar, V.J. Shukla, Indian systems of medicine: A brief profile, African J. Tradit. Complement. Altern. Med., 2007, 4, 319– 337. https://doi.org/10.4314/AJTCAM.V4I3.31226.
- P.K. Sarkar, A. Wele, Presence and activities of carbonaceous nanomaterials in Ayurvedic nano-medicine preparations, *Int. Nano Lett.*, 2023, 13, 41–51. https://doi.org/10.1007/S40089-022-00383-Z/METRICS.
- K.E. Jawale, A. Rakibe, Concept of Bhasma, their Preparation and Significance in Rasashastra, *Himal. J. Heal. Sci.*, 2025, 9–11. https://doi.org/10.22270/HJHS.V10I1.223.
- A.A.L. Michalchuk, E. V. Boldyreva, A.M. Belenguer, F. Emmerling, V. V. Boldyrev, Tribochemistry, Mechanical Alloying, Mechanochemistry: What is in a Name?, Front. Chem., 2021, 9, 685789. https://doi.org/10.3389/FCHEM.2021.685789.
- K.D. Yadav, A.K. Chaudhary, A.K. Verma, Bioavailability Enhancement of Partially Water Soluble Solid Medicament in Traditional System of Medicine, *Indian J. Pharm. Sci.*, 2017, 79, 667–673. https://doi.org/10.4172/PHARMACEUTICAL-
- SCIENCES.1000278.

 10. T. Tsuzuki, Mechanochemical synthesis of metal oxide nanoparticles, *Commun. Chem.* 2021 41, 2021, 4, 1–11.
- https://doi.org/10.1038/s42004-021-00582-3.
 11. T. Tsuzuki, P.G. McCormick, Mechanochemical synthesis of nanoparticles, *J. Mater. Sci.*, 2004, 39, 5143–5146.
 https://doi.org/10.1023/B:JMSC.0000039199.56155.F9.
- S. Pal, The Ayurvedic Bhasma: The Ancient Science of Nanomedicine, *Recent Patents Nanomed.*, 2015, 5, 12–18. https://doi.org/10.2174/1877912305666150417233945.
- J. Zhang, K. Hu, L. Di, P. Wang, Z. Liu, J. Zhang, P. Yue, W. Song, J. Zhang, T. Chen, Z. Wang, Y. Zhang, X. Wang, C. Zhan, Y.C. Cheng, X. Li, Q. Li, J.Y. Fan, Y. Shen, J.Y. Han, H. Qiao, Traditional herbal medicine and nanomedicine: Converging disciplines to improve therapeutic efficacy and human health, Adv. Drug Deliv. Rev., 2021, 178, 113964. https://doi.org/10.1016/J.ADDR.2021.113964.
- E. Figueiredo, Optical Microscopy, Encycl. Archaeol. Sci., 2018, 1– 4. https://doi.org/10.1002/9781119188230.SASEAS0422.
- A. Sharma, E.G. Naz, S. SIngh, K. Tripathi, Fundamental concepts of spectroscopy and spectrometry for chemical analysis, Career Point Ltd., n.d.
- D.K. PG, N.Y. P., G.S., N.K.S., Analytical Methods in Standardization of Bhasmas: A Review, *J. Drug Deliv. Ther.*, 2021, 11, 183–192. https://doi.org/10.22270/JDDT.V1115.4960.
- T.S. Soliman, Effects of SiO2 Nanoparticles on Polyvinyl Alcohol/Carboxymethyl Cellulose Polymer Blend Films' Structural, Wettability, Surface Roughness, and Optical Characteristics, *Adv. Polym. Technol.*, 2024, 2024, 3623198. https://doi.org/10.1155/2024/3623198.
- S. Kantak, N. Rajurkar, P. Adhyapak, Synthesis and characterization of Abhraka (mica) bhasma by two different methods, *J. Ayurveda Integr. Med.*, 2020, 11, 236–242. https://doi.org/10.1016/J.JAIM.2018.11.003.
- A. Wele, S. De, M. Dalvi, N. Devi, V. Pandit, Nanoparticles of biotite mica as Krishna Vajra Abhraka Bhasma: synthesis and characterization, *J. Ayurveda Integr. Med.*, 2021, 12, 269–282. https://doi.org/10.1016/J.JAIM.2020.09.004.
- F. Hashem, M. Nasr, Y. Ahmed, Preparation and Evluation of Iron Oxide Nanoparticles for Treatment of Iron Deficiency in Anemia, *Int. J. Pharm. Pharm. Sci.*, 2018, 10, 142. https://doi.org/10.22159/IJPPS.2018V10I1.22686.
- M.M. Ba-Abbad, M.S. Takriff, A. Benamor, A.W. Mohammad, Size and shape controlled of α-Fe2O3 nanoparticles prepared via sol–gel technique and their photocatalytic activity, *J. Sol-Gel Sci. Technol.*, 2017, 81, 880–893. https://doi.org/10.1007/S10971-016-4228-4.
- G. D, Comparative characterization study of Loha Bhasma and Triphala derived Iron Nano Particles, *J. Ayurveda Integr. Med. Sci.*, 2024, 9, 67–72. https://doi.org/10.21760/JAIMS.9.6.9.

- S. Yadav, Synthesis And Characterization Of Ayurvedic Loha Bhasma (Powder) By Different Method, *Int. J. Creat. Res. Thoughts*, 2025, 13, 528–535. https://www.ijcrt.org/papers/IJCRT2503874.pdf.
- V. Jadhav, A. Bhagare, S. Wahab, D. Lokhande, C. Vaidya, A. Dhayagude, M. Khalid, J. Aher, A. Mezni, M. Dutta, Green Synthesized Calcium Oxide Nanoparticles (CaO NPs) Using Leaves Aqueous Extract of Moringa oleifera and Evaluation of Their Antibacterial Activities, J. Nanomater., 2022, 2022, 9047507. https://doi.org/10.1155/2022/9047507.
- N. Lalou, A. Kadari, Influence of Li2+ Doping on the Structural and Optical Properties of CaO Synthesized by Sol–Gel Process, *J. Mol. Eng. Mater.*, 2019, 07,. https://doi.org/10.1142/S2251237319500023.
- A. Mishra, A.K. Mishra, O.P. Tiwari, S. Jha, In-house preparation and characterization of an Ayurvedic bhasma: Praval bhasma, J. Integr. Med., 2023, 12, 52–58. https://doi.org/10.1016/S2095-4964(14)60005-4.
- P. KC, V. G, R. MD, Preparation and Physiochemical Characterization of Indian Traditional Medicine: Praval Bhasma by using Modern Analytical Techniques, *Int. J. Pharma Res. Technol.*, 2010, 2, 101–08. https://www.ijprt.com/uploads/menuscript/9a7bfda00297e0991487
 - https://www.ijprt.com/uploads/menuscript/9a7bfda00297e0991487dc431162053a.pdf.
- Calcite Database of ATR-FT-IR spectra of various materials, n.d.,. https://spectra.chem.ut.ee/paint/fillers/calcite/ (accessed July 27, 2025).
- S. Singh, A. Bharti, V.K. Meena, Green synthesis of multi-shaped silver nanoparticles: optical, morphological and antibacterial properties, *J. Mater. Sci. Mater. Electron.*, 2015, 26, 3638–3648. https://doi.org/10.1007/S10854-015-2881-Y.
- A.S. Gungure, L.T. Jule, N. Nagaprasad, K. Ramaswamy, Studying the properties of green synthesized silver oxide nanoparticles in the application of organic dye degradation under visible light, *Sci. Rep.*, 2024, 14, 1–23. https://doi.org/10.1038/S41598-024-75614-8.
- M.D. Bhavani, M. Raju, C. Sridurga, K.V. Subbaiah, Analytical Standardization of Rajata Bhasma, *Int. J. Res. AYUSH Pharm. Sci.*, 2018, 2, 229–238.
 - https://www.ijraps.in/index.php/ijraps/article/view/39 (accessed July 27, 2025).
- K. Kalimuthu, J.M. Kim, C. Subburaman, W.Y. Kwon, S.H. Hwang, S. Jeong, M.G. Jo, H.J. Kim, K.S. Park, Characterization of Rajath Bhasma and Evaluation of Its Toxicity in Zebrafish Embryos and Its Antimicrobial Activity, *J. Microbiol. Biotechnol.*, 2020, 30, 920– 925. https://doi.org/10.4014/JMB.1911.11018.
- S. Chavan, S. Tayade, V. Gupta, V. Deshmukh, S. Sardeshmukh, Pharmaceutical Standardization and Physicochemical Characterization of Traditional Ayurvedic Marine Drug: Incinerated Conch Shell (Shankha Bhasma), Mar. Drugs, 2018, 16, 450. https://doi.org/10.3390/MD16110450.
- S. Savita, Y. Yadevedra, S. Usha, R. Sushma, S. Khemchand, Characterization of Conch Shell Nanoparticles (Shanka Bhasma) Synthesized by the Classical Method, Sch. Int. J. Tradit. Complement. Med., 2020, 03, 90–99. https://doi.org/10.36348/SIJTCM.2020.V03I05.002.
- Y. Yuan, L. Wang, L. Gao, Nano-Sized Iron Sulfide: Structure, Synthesis, Properties, and Biomedical Applications, *Front. Chem.*, 2020, 8, 818. https://doi.org/10.3389/FCHEM.2020.00818.
- P.A. Ajibade, N.L. Botha, Synthesis and structural studies of copper sulfide nanocrystals, *Results Phys.*, 2016, 6, 581–589. https://doi.org/10.1016/J.RINP.2016.08.001.
- A.M. Paca, P.A. Ajibade, Synthesis, Optical, and Structural Studies of Iron Sulphide Nanoparticles and Iron Sulphide Hydroxyethyl Cellulose Nanocomposites from Bis-(Dithiocarbamato)Iron(II) Single-Source Precursors, Nanomaterials, 2018, 8, 187. https://doi.org/10.3390/NANO8040187.
- M.A. Martuza, S. Pokhrel, J. Stahl, M. Schowalter, A. Rosenauer, L. Mädler, Controlled Synthesis of Copper Sulfide Nanoparticles in Oxygen-Deficient Conditions Using Flame Spray Pyrolysis (FSP) and Its Potential Application, Small, 2025, 21, 2409993. https://doi.org/10.1002/SMLL.202409993.

Advanced Materials Letters

https://aml.iaamonline.org

OPEN ACCESS

- S. Yadav, V. Choudhary, Synthesis And Characterization Of Ayurvedic Suvarnamakshik Bhasma (Powder) By Different Method, Int. J. Creat. Res. Thoughts, 2025, 13, 552–562. https://www.ijcrt.org/papers/IJCRT2501513.pdf.
- D. Varghese, C. Tom, N. Krishna Chandar, Effect of CTAB on structural and optical properties of CuO nanoparticles prepared by coprecipitation route, *IOP Conf. Ser. Mater. Sci. Eng.*, 2017, 263, https://doi.org/10.1088/1757-899X/263/2/022002.
- A.M. Al-Fa'ouri, O.A. Lafi, H.H. Abu-Safe, M. Abu-Kharma, Investigation of optical and electrical properties of copper oxide polyvinyl alcohol nanocomposites for solar cell applications, *Arab. J. Chem.*, 2023, 16, 104535. https://doi.org/10.1016/J.ARABJC.2022.104535.
- R.K. Singh, S. Kumar, A.K. Aman, S.M. Karim, S. Kumar, M. Kar, Study on physical properties of Ayurvedic nanocrystalline Tamra Bhasma by employing modern scientific tools, *J. Ayurveda Integr.* Med., 2019, 10, 88–93. https://doi.org/10.1016/J.JAIM.2017.06.012.
- G.M. Kamel, M.N. El-Nahass, M.E. El-Khouly, T.A. Fayed, M. El-Kemary, Simple, selective detection and efficient removal of toxic lead and silver metal ions using Acid Red 94, RSC Adv., 2019, 9, 8355–8363. https://doi.org/10.1039/C9RA00464E.
- L. Das, L.D. Koonathan, A. Kunwar, S. Neogy, A.K. Debnath, S. Adhikari, Nontoxic photoluminescent tin oxide nanoparticles for cell imaging: deep eutectic solvent mediated synthesis, tuning and mechanism, *Mater. Adv.*, 2021, 2, 4303–4315.

SUPPORTING INFORMATION

Supporting Table S1. Summary of the average particle size, UV-vis absorbance, band gap energy and FTIR analysis results of commercial Bhasmas.

Bhasmas	Optical image Av. particle size (μm)	UV-vis spectrum		FTIR spectrum		
		Wavel ength (nm)	Band gap energy (eV)	Remarks	Wave- number (cm ⁻¹)	Remarks
Abhrak	28.5	257	3.01	Nanosize d silicate	2920, 1850, 1745, 952	Mg-OH, Al- OH, O=C=O, Si-O stretching vibrations
Loha	23.5	336	5.12	Iron oxide NPs	526, 432	Fe-O bonds
Praval	20.1	335	4.65	CaO NPs	3690, 2520, 1795, (1400, 873, 710)	O-H, C-H, C- O stretching vibrations, Asymmetric carbonate of calcite
Rajat	31.2	338	1.94	Impuritie s other than Ag NPs	3900- 3700, 1460, 408	O-H stretching, CH ₂ bending, Ag-O bond
Sankha	14.7	336	4.85	CaO NPs	3640, (1415, 874, 712), 425	O-H stretching, Asymmetric carbonate of calcite
Suvarna makshik	30.0	310	5.25	FeS and CuS NPs	1069, 528, 439	C-O stretching, Fe-O, Cu-O bonds
Tamra	18.6	340	5.36	CuO NPs	3735, 1056, 430	O-H stretching, C- O stretching, Cu-O bond
Trivanga	37.2	214, 248, 322	5.35	Nanosize d Pb, Sn and Zn compoun ds	2340, 1463, 1039, 593, 471	CO ₂ molecule, CH ₂ bending, C-O stretching, Sn-O, Cu-O bond
Vanga	30.5	290, 390	4.47	SnO ₂ and CuO NPs	605, 459	Sn-O, Cu-O bonds
Yashad	28.0	347	4.85	ZnO NPs	1486, 887, 419	CH ₂ bending, C-O stretching, Zn-O bond

- https://doi.org/10.1039/D1MA00042J.
- D.K. Singh, D.K. Pandey, R.R. Yadav, D. Singh, A study of nanosized zinc oxide and its nanofluid, *Pramana - J. Phys.*, 2012, 78, 759–766. https://doi.org/10.1007/S12043-012-0275-8.
- S.D. Meshram, R. V Rupnarayan, S. V Jagtap, V.G. Mete, V.S. Sangawar, Synthesis and Characterization of Lead Oxide Nanoparticles, 2015, 4, 83–88.
- P.A. Luque, O. Nava, C.A. Soto-Robles, H.E. Garrafa-Galvez, M.E. Martínez-Rosas, M.J. Chinchillas-Chinchillas, A.R. Vilchis-Nestor, A. Castro-Beltrán, SnO2 nanoparticles synthesized with Citrus aurantifolia and their performance in photocatalysis, *J. Mater. Sci. Mater. Electron.*, 2020, 31, 16859–16866. https://doi.org/10.1007/S10854-020-04242-5.
- M. Junaid, S. Ghulam Hussain, N. Abbas, W.Q. khan, Band gap analysis of zinc oxide for potential bio glucose sensor, *Results Chem.*, 2023, 5, 100961. https://doi.org/10.1016/J.RECHEM.2023.100961.
- B. Kale, N. Rajurkar, Synthesis and characterization of Vanga bhasma, J. Ayurveda Integr. Med., 2019, 10, 111–118. https://doi.org/10.1016/j.jaim.2017.05.003.
- A. Balkrishna, D. Sharma, R.K. Sharma, K. Bhattacharya, A. Varshney, Investigating the Role of Classical Ayurveda-Based Incineration Process on the Synthesis of Zinc Oxide Based Jasada Bhasma Nanoparticles and Zn2+ Bioavailability, ACS Omega, 2023, 8, 2942–2952. https://doi.org/10.1021/ACSOMEGA.2C05391.



This article is licensed under a Creative Commons Attribution 4.0 International License, which allows for use, sharing, adaptation, distribution, and reproduction in any medium or format, as long as appropriate credit is given to the original author(s) and the source, a link to the Creative Commons license is provided, and changes are indicated. Unless otherwise indicated in a credit line to the materials, the images or other third-party materials in this article are included in the article's Creative Commons license. If the materials are not covered by the Creative Commons license and your intended use is not permitted by statutory regulation or exceeds the permitted use, you must seek permission from the copyright holder directly.

Visit http://creativecommons.org/licenses/by/4.0/ to view a copy of this license

GRAPHICAL ABSTRACT

